The petrology and significance of a stratiform mafic segregation pegmatite in a Karoo-aged dolerite sheet

A.A. Mitchell+ and S.B. Naicker*

Department of Geology, University of Durban-Westville, Private Bag X54001, Durban, 4000 Republic of South Africa

J.S. Marsh

Department of Geology, Rhodes University, Grahamstown, 6140 Republic of South Africa

J.N. Dunlevey

Department of Geology, University of Durban-Westville, Private Bag X54001, Durban, 4000 Republic of South Africa

Accepted 21 May 1997

A sub-horizontal stratiform mafic segregation pegmatite, of the order of 30 cm thick, occurs within 25 m of the top contact of a Karoo-aged dolerite sheet at Pietermaritzburg, South Africa. The host rock is an orthopyroxene-rich dolerite containing 5 – 8% interstitial granophyre. The pegmatite is similar to the host dolerite in many respects, except that the granophyre content is higher, and acicular augite is the only pyroxene. At its upper contact, a laterally continuous sub-horizontal joint forms a sharp boundary to the pegmatite, whilst the lower contact is gradational over a few millimetres. Low MgO and chalcophiles, and elevated incompatible element contents, are the main geochemical attributes of the pegmatite. The footwall of the stratiform pegmatite is characterized by slightly elevated incompatible element contents up to 0.74 m from the contact, and small, irregular pods of pegmatite occur within 0.5 m of the main pegmatite layer. In the hanging-wall dolerite, incompatible element enrichment is confined to within 0.3 m of pegmatite. Inter-element plots of the incompatible elements (TiO_2, Zr, and Y) and compatible elements (MgO, Cr, and Ni) produce linear regression lines with correlation coefficients of 0.98 or better, indicating the consanguinity of the hanging-wall and footwall dolerites and the enclosed pegmatite, with no evidence for assimilation of country rock material. The pegmatite represents an estimated 25 to 35% fractionation of the dolerite, which accords with the results of comparable studies on similar bodies of rock. In common with other documented cases, the pegmatite is situated within the upper 50% of the intrusion. Although segregation may have taken place within a single intrusion, the sharp, jointed upper contact suggests that the pegmatite could have accumulated at the interface between a new influx of magma and the overlying, partially crystalline, products of an earlier influx within a multiple intrusion. Pegmatites in small intrusions of the type described here are considered to be incipient forms of the more complexly evolved pegmatites found in large layered intrusions.

'n Subhorisontale, laagvormige, mafiese segregasiepegmatiet, ongeveer 30 cm dik, kom binne 25 cm vanaf die bo-kontak van 'n dolerietplaat van Karoo-ouderdom te Pietermaritzburg, Suid-Afrika, voor. Die herberggesteente is doleriet, ryk aan ortopirokseen, en bevat 5 – 8% interstitiële granofier. Die pegmatiet is in vele opsigte soortgelyk aan die herbergdoleriet, behalwe dat die granofierinhoud hoër is en naaldvormige ougiet die enigste pirokseen is. 'n Lateraalaaneenopende, subhorisontale naat vorm 'n skerp grens met die pegmatiet by die bo-kontak, terwyl die laer oorgangskontak oor 'n aantal millimeter strek. Die vernaamste geochemiese kenmerke van die pegmatiet is lae MgO en chalkofiele, en verhoogde onversoenbare elementinhoud. Die vloer van die gelaagde pegmatiet word gekenmerk deur effens verhoogde onversoenbare elementinhoud tot 0.74 m vanaf die kontak; en klein onreëlmatige pegmatietpeule kom binne 0.5 m vanaf die hoof pegmatietlaag voor. In die dakdoleriet is onversoenbare elementverryking beperk tot binne 0.3 m vanaf die pegmatiet. Interelement-stipdiagramme van die onverenigbare elemente (TiO_2, Zr, en Y) en versoenbare elemente (MgO, Cr, en Ni) lewer lineêre regressielyne met korrelasiekoëffisiënte van 0.98 of beter op, wat die stamverwantskap van die dak- en vloerdoleriete en die ingeslote pegmatiet aandui, met geen teken van die assimilasie van newegesteentemateriaal nie. Die pegmatiet verteenwoordig 'n beraamde 25 tot 35% fraksionering van die doleriet, wat ooreenstem met die resultate van vergelykbare navorsing op soortgelyke gesteenteliggame. Die pegmatiet is geleë binne die boonste 50% van die intrusie, net soos dit in die ander gedokumenteerde studies die geval is. Die skerp, genate bo-kontak dui daarop dat die pegmatiet by die grensvlak tussen 'n nuwe instroming van magma en die oorliggende, gedeeltelik kristallyne, produkte van 'n vroeëre instroming binne 'n veelvoudige indringing, kon opgehoop het; hoewel die segregasie ook binne 'n enkele intrusie kon plaasgevind het. Pegmatiete in klein intrusies, soos die tipe wat hier beskryf word, word beskou as aanvangsvorme van die meer kompleksontwikkelde pegmatiete wat in groot gelaagde intrusies aangetref word.

+Corresponding author: E-mail address mitchell@pixie.udw.ac.za

*Present address: Geology Department, New Vaal Colliery, Private Bag X414, Viljoensdrif, 9580 Republic of South Africa

Introduction

Coarse-grained, mafic segregation pegmatite, often with a high percentage of interstitial granophyric material, is common within thick tholeiitic lava flows (Puffer & Horter, 1993; Philpotts *et al.*, 1996), and in thick dolerite sheets like the Whin Sill in northern England (Randall, 1989), the Pallisades Sill in New Jersey, USA (Shirley, 1987), intrusives in the Jurassic Ferrar Province of Antarctica (Wilhelm & Wörner, 1996), and in various intrusions of Karoo dolerite in southern Africa (Walker & Poldervaart, 1949; Eales, 1959; Mountain, 1960; Eales & Booth, 1974; Williams, 1995; Encarnación *et al.*, 1996). In large layered mafic intrusions like the Skaergaard Complex in Greenland, the development of pegmatites is advanced to the extent that an evolutionary trend is evident

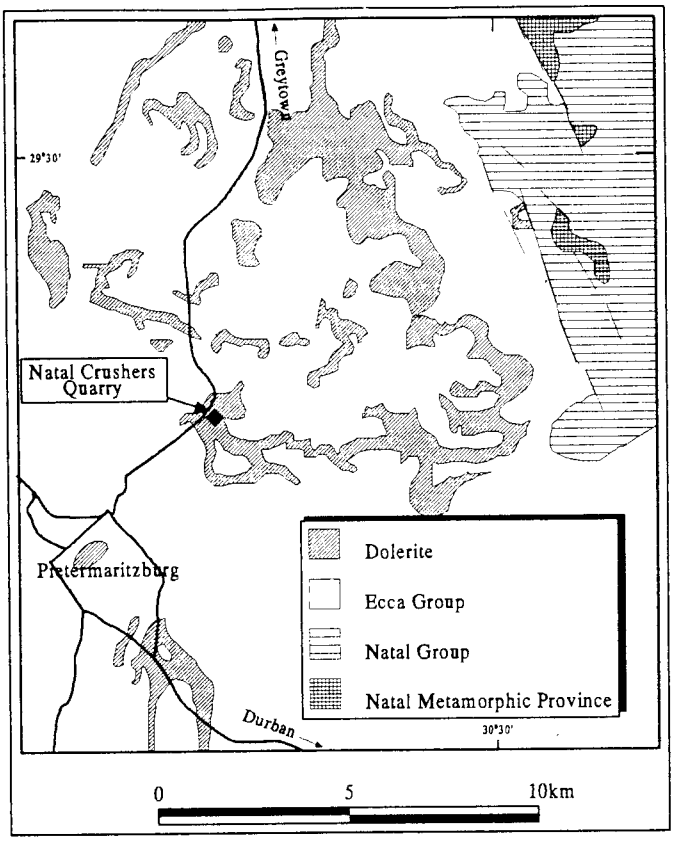

Figure 1 Locality map of the Pietermaritzburg area, showing the site of the Natal Crushers Quarry (simplified after Linström, 1987).

in the petrology and geometry of these bodies from bottom to top of the intrusion, as well as within individual pegmatite bodies (Larsen & Brooks, 1994). In the Bushveld Complex in South Africa, the largest known layered tholeiitic complex in the world, pods, pipes, and sheets of iron-rich ultramafic pegmatite (Scoon & Mitchell, 1994) form an extreme case of pegmatite segregation from a mafic body, although in these latter bodies there is also a component of replacement.

Segregation pegmatites in relatively small mafic bodies are not strongly evolved by comparison with those in the large layered complexes. They are, however, perhaps significant in that they represent early manifestations of processes that develop to their fullest extent in the largest of mafic intrusions.

The stratiform segregation pegmatite described here occurs within a dolerite sheet currently being exploited by the Anglo Alpha group at the Natal Crushers Quarry in Pietermaritzburg (Figure 1). Many segregation pegmatites show evidence of having formed by migration of late-stage liquids into the upper 50% of a single cooling unit, that is, a single lava flow or dolerite intrusion (Puffer & Horter, 1993; Philpotts *et al.*, 1996), or the interior of a single injection of magma within an intrusive sheet that shows evidence of multiple intrusion (Shirley, 1987). In the Whin Sill in England, semi-conformable pegmatite lenses formed near the top of the intrusion (Tomkeieff, 1929; Randall, 1989). In the case investigated here, pegmatite could have formed within a single intrusion, but there is some evidence for the involvement of two successive, contiguous injections of magma in a composite dolerite sheet, with the pegmatite forming at the contact between the two magma batches.

Geological setting

The Natal Crushers Quarry is situated on the New Greytown road, on the eastern outskirts of Pietermaritzburg (Figure 1). Quarrying operations are centred on a dolerite sheet with an exposed thickness of slightly more than 80 m. The upper contact of the sheet with shales of the Permian Pietermaritzburg Formation (Ecca Group) is exposed in the quarry, but its lower contact is not exposed. The pegmatite occurs as a subhorizontal stratiform layer, between 5 and 30 cm thick, at a depth of between 25 m and 40 m below the top contact of the sheet, and is exposed only on the southern and southwestern walls of the quarry, where it can be traced laterally for a distance of approximately 150 m. The upper contact of the pegmatite is marked by a laterally continuous horizontal joint. The lower contact with the host dolerite, by contrast, is horizontally jointed in places only, and is generally sharp or else gradational over a few millimetres. In the footwall, isolated small (less than 0.5 m long) pods of pegmatite occur in the dolerite within 0.5 m of the main stratiform pegmatite body.

Sampling and analytical techniques

Sampling was concentrated around the pegmatite and its immediate footwall and hanging wall, and only relatively few samples were collected from benches above and below that on which the pegmatite is exposed. Samples SB1, SB2, and SB3 are from the hanging-wall dolerite. SB1 was taken from a bench 14.6 m above the pegmatite, and SB2 and SB3 within 0.5 m of the hanging-wall contact of the pegmatite. Samples SB4, SB5, and SB6 are from the main segregation pegmatite layer, and sample SB13 is from a small pegmatite pod below the main pegmatite. SB7, SB8, SB9, SB10, and SB11 are all from the footwall dolerite within 1 m of the segregation pegmatite, and sample SB12 is host dolerite from a bench 14 m below the pegmatite.

Whole-rock major-element determinations were performed at Rhodes University, using the fusion technique of Norrish & Hutton (1969), and sodium and the trace elements were determined on undiluted pressed powder pellets. Loss on ignition (LOI) and H_2O^- were determined gravimetrically. CIPW norms were calculated from normalized anhydrous whole-rock major-element data, assuming a ratio Fe_2O_3/FeO of 0.15. Mineral analyses were performed at the University of Durban-Westville, using a JEOL JSM-6100 scanning electron microscope (SEM), equipped with a NORAN Voyager energy-dispersive spectrometer (EDS) and ZAF data correction software. The SEM was operated at 20 kV, with a beam current of 0.22 nA measured on a Faraday cage. Counting times of 200 seconds were employed, and calibration was by means of a wollastonite standard for Ca and Si, NaCl for Na, microcline for K, and pure element standards for the remaining elements. Backscattered electron (BSE) images were also obtained from the JEOL JSM-6100.

Petrography and mineral proportions

Host dolerite

The chilled top contact of the dolerite sheet contains isolated subhedral to euhedral orthopyroxene and plagioclase phenocrysts in a fine-grained groundmass (Figure 2a). The body of the dolerite sheet, both in the footwall and in the hanging wall of the pegmatite, conforms most closely to the type referred to by Walker & Poldervaart (1949, p. 616) as the 'Hangnest Type', an orthopyroxene dolerite in which zoned plagioclase occurs with subophitic to poikilitic augite (Figures 2b, c, and d), some of the latter containing pigeonite cores. Orthopyroxene differs from augite in generally forming slightly smaller grains, and in being consistently subhedral and non-ophitic (Figure 2d). Iron-enrichment along grain margins is a feature of both orthopyroxene and augite. Abundant interstitial granophyre, an intergrowth of quartz and alkali feldspar (Figure 2a), contains scattered fine, acicular grains of apatite. The presence of the interstitial granophyre is reflected in CIPW normative quartz contents of between 4 and 5% in the host dolerite (Table 1). The alkali feldspar in the interstitial granophyre varies from pure K-feldspar to a K-feldspar/albite microperthite. The content of sulphide and oxide minerals in the dolerite is low (generally less than 3.5%), which contributes to the quality of the rock as an aggregate. Modal analyses of selected samples conform very closely with the CIPW normative mineralogy, and so mineral proportions in this discussion are based for the most part on normative data.

The total pyroxene content of the host dolerite is generally between 39.3% and 42.1%. The exception is sample SB12, the lowermost sample in the footwall dolerite, in which the total normative pyroxene content is 46.7%. The normative orthopyroxene content of SB12 is 35.41%, which accords closely with a point-counted modal determination of 34.4% orthopyroxene. Excluding sample SB12, which is more primitive in several respects than all the other samples, there is a definite difference between the hanging-wall dolerite, with a range of 27.8 to 28.9% normative orthopyroxene, and the footwall dolerite, with a range of 24.14 to 26.64%. This is confirmed by modal determinations. The normative ratio hyen/(hyen+hyfs), an indicator of the composition of the orthopyroxene, is a consistent 0.57 in the hanging-wall dolerite, and ranges from 0.58 to 0.60 in the footwall, once again with the exception of the relatively mafic sample SB12 (0.65). Although pyroxene proportions and compositional ratios show the footwall dolerite to be more primitive than the hanging-wall, the reverse is true of plagioclase compositions, with

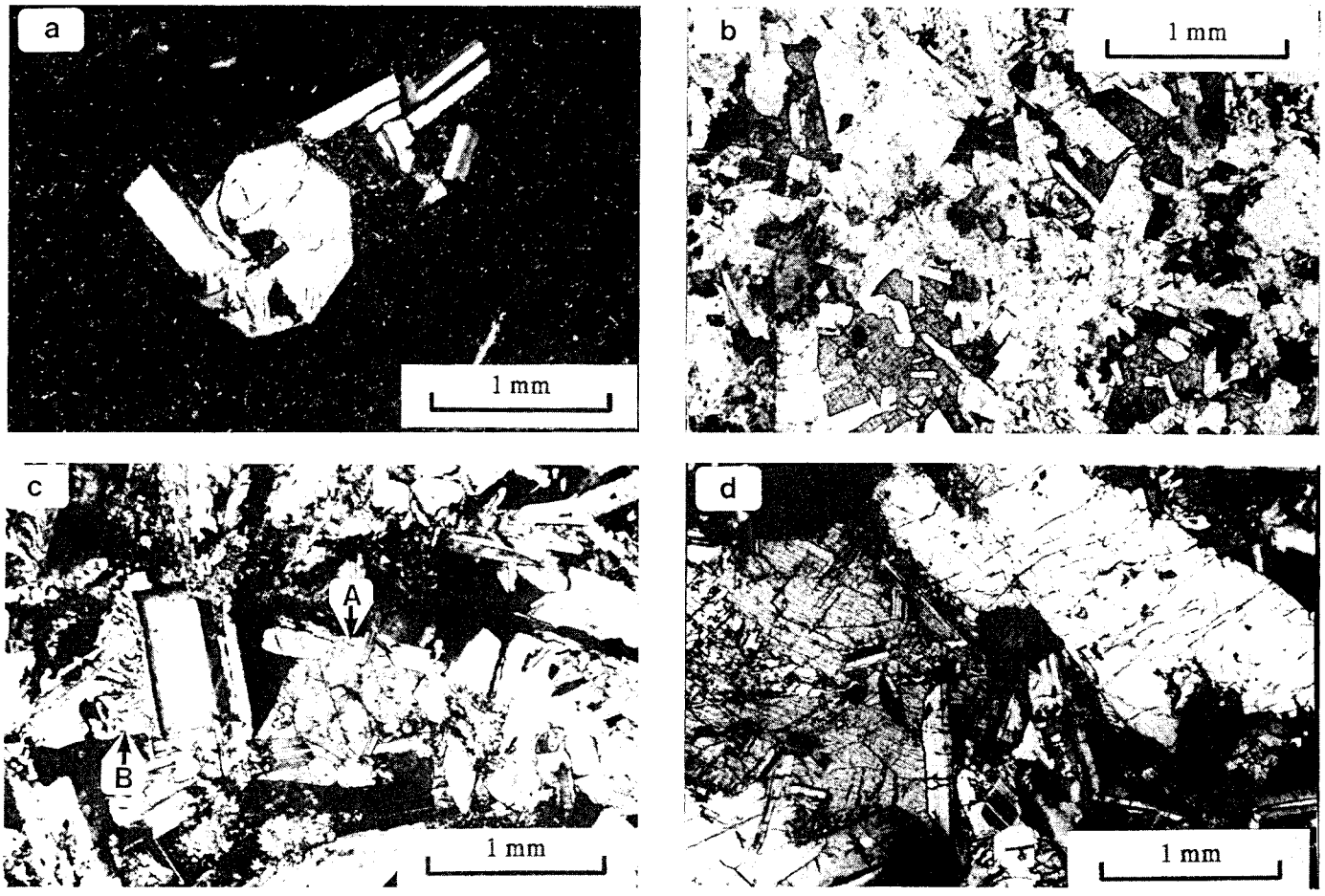

Figure 2 Photomicrographs of dolerite hosting the segregation pegmatite. **a)** Subhedral orthopyroxene and plagioclase crystals in fine-grained intersertal groundmass, upper chilled margin of hanging-wall dolerite (crossed polars). **b)** Poikilophitic augite (dark grey) and plagioclase (pale grey) in sample SB3, hanging-wall dolerite close to the upper contact of the pegmatite (plane polarized light). **c)** Ophitic augite (A) and interstitial granophyre (B) in sample SB7, footwall dolerite close to the pegmatite contact (crossed polars). **d)** Poikilophitic augite (mid-grey, left of field of view) and non-ophitic orthopyroxene (pale grey, right of field of view), sample SB12, footwall dolerite (crossed polars).

Table 1 CIPW norms

SAMPLE	SB1	SB2	SB3	SB4	SB5	SB6	SB7	SB8	SB9	SB10	SB11	SB12	SB13
ap	0.24	0.26	0.27	0.48	0.51	0.41	0.31	0.27	0.24	0.27	0.29	0.26	0.41
il	1.42	1.42	1.47	2.61	2.63	2.17	1.56	1.53	1.54	1.51	1.46	1.39	2.01
or	4.55	4.37	3.92	5.72	5.82	4.93	4.84	4.33	4.55	4.63	4.07	3.48	3.63
ab	21.19	21.17	19.84	24.90	24.05	24.81	22.25	21.44	21.85	21.78	20.59	19.58	20.38
an	27.09	27.30	26.08	17.00	22.04	22.90	25.10	26.48	24.90	25.55	24.95	22.63	25.49
mt	1.96	1.92	2.02	2.45	2.10	2.04	1.86	1.82	1.86	1.83	1.84	1.95	1.91
dien	3.29	3.26	3.43	4.05	2.87	3.80	4.21	4.54	4.31	4.19	4.55	3.54	4.28
difs	2.50	2.42	2.57	5.78	4.15	4.23	3.07	3.25	3.06	2.97	3.00	1.94	4.34
diwo	6.01	5.90	6.23	9.77	6.98	8.12	7.57	8.12	7.68	7.46	7.90	5.80	8.78
hyen	15.80	15.92	16.51	8.15	7.22	9.16	14.43	14.07	14.89	14.66	16.06	22.88	9.13
hyfs	12.00	11.81	12.40	11.64	10.44	10.22	10.53	10.07	10.57	10.41	10.58	12.53	9.27
q	3.96	4.24	5.26	7.46	11.20	7.23	4.28	4.10	4.55	4.76	4.71	4.01	10.38
TOTAL	100.01	100.01	100.01	100.01	100.01	100.01	100.01	100.01	100.01	100.01	100.01	100.01	100.01
An/(Ab +An)	0.56	0.56	0.57	0.41	0.48	0.48	0.53	0.55	0.53	0.54	0.55	0.54	0.56
Total plag	48.28	48.47	45.92	41.90	46.09	47.71	47.35	47.92	46.75	47.33	45.54	42.21	45.87
Total px	39.60	39.31	41.14	39.39	31.66	35.53	39.81	40.05	40.51	39.69	42.09	46.69	35.80
Total opx	27.80	27.73	28.91	19.79	17.66	19.38	24.96	24.14	25.46	25.07	26.64	35.41	18.40
hyen/(hyen+hyfs)	0.57	0.57	0.57	0.41	0.41	0.47	0.58	0.58	0.58	0.58	0.60	0.65	0.50
mt/(mt+ il)	0.58	0.57	0.58	0.48	0.44	0.48	0.54	0.54	0.55	0.55	0.56	0.58	0.49

ap = apatite
il = ilmenite
or = orthoclase
ab = albite
an = anorthite
dien = diopside (enstatite component)
difs = diopside (ferrosilite component)
diwo = diopside (wollastonite component)
hyen = hypersthene (enstatite component)
hyfs = hypersthene (ferrosilite component)
mt = magnetite
q = quartz
Total plag = ab+an
Total px = dien+difs+diwo+ hyen+hyfs
Total opx = hyen+hyfs

the normative ratio An/(An+Ab) in the range 0.56 – 0.57 in the hanging wall, and 0.53 – 0.55 in the footwall, even including sample SB12 (Table 1). The normative ratio magnetite/(magnetite+ilmenite) also distinguishes the hanging wall (range 0.57 – 0.58) from the footwall (0.54 – 0.56), sample SB12 again being the exception for footwall compositions (0.58). Normative data relating to pyroxene and magnetite should, however, be used with some caution, since they are based on a constant and theoretical iron oxidation ratio.

Segregation pegmatite

The segregation pegmatite contains a similar mineral assemblage to the host dolerite, except that orthopyroxene and pigeonite are absent, there is a greater development of interstitial granophyre (reflected in a normative quartz content of between 7 and 11%), and hydrous phases are more abundant, most specifically in the form of partial secondary amphibole (uralite) replacement of augite. Augite grains, which may reach 7 mm in length, are characteristically curved and have

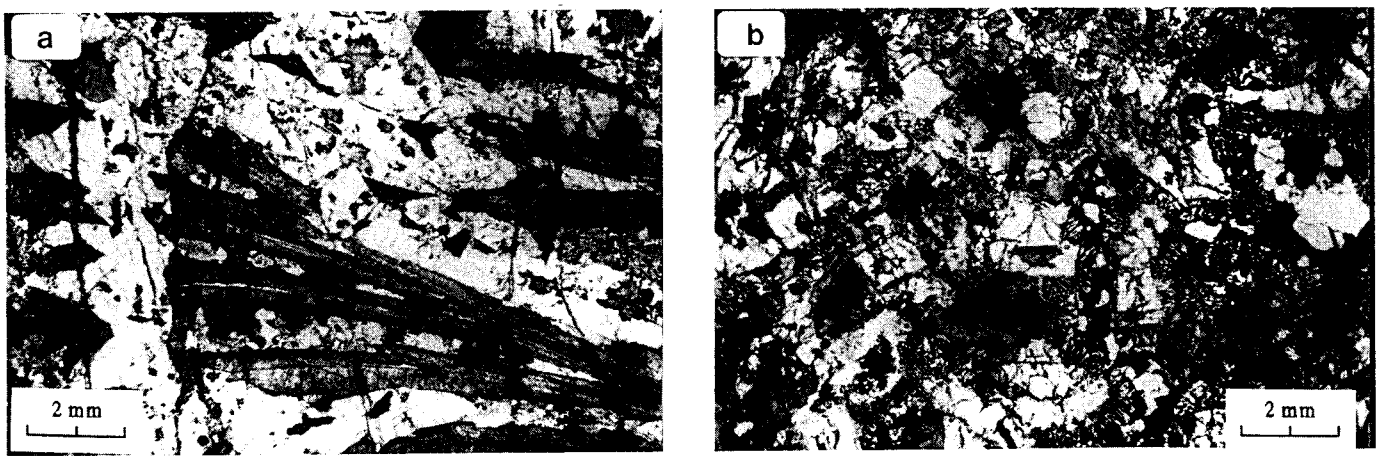

Figure 3 Photomicrographs of dolerite segregation pegmatite. **a)** Elongate, curved augite grains, sample SB13 (plane polarized light). **b)** Substantial development of interstitial granophyre, sample SB6 (crossed polars).

conspicuous median twin planes (Figure 3a). Marginal iron-enrichment of augite grains is common (Figure 4a), and some grains have iron-rich cores (Figure 4b). Where augite is uralitized, relict skeletal ilmenite exsolution lamellae, remaining after alteration of the original magnetite host, may form geometric patterns in the fine-grained hornblende (Figure 4c). Such replacement of magnetite under the relatively hydrous conditions pertaining to doleritic pegmatites has also been documented in the Palisades Sill (Shirley, 1987). The granophyre is host to a variety of accessory phases, most conspicuously apatite, some of which occurs as overgrowths on tiny euhedral quartz grains (Figure 4d). Other accessory phases, in many cases so fine-grained that they are only distinguishable under the electron microscope, include sphene, baddeleyite (ZrO_2), and zircon (Naicker, 1996). Sulphides are present in small amounts, the most common being pyrite and chalcopyrite, with isolated occurrences of sphalerite. In common with other pegmatites, whether granitic (e.g. Jahns & Burnham, 1969), mafic (Puffer & Horter, 1993; Larsen & Brooks, 1994), or even ultramafic (Scoon & Mitchell, 1994), the pegmatite described here is heterogeneous, both in terms of mineralogy and of grain size. The elongated augite grains, for example, are not ubiquitous, and the proportion of interstitial granophyre (Figure 3b) varies considerably within the body.

Whole-rock chemistry

Host dolerite

Several chemical parameters define differences between the hanging-wall and footwall dolerite (Figure 5). The hanging-wall dolerite is most clearly distinguished from the footwall dolerite by consistently higher Cu concentrations (in excess of 90 ppm, as opposed to 80 ppm or less in the footwall). Co decreases from a concentration of 53 ppm in sample SB12, 14 m below the pegmatite, to between 44 and 46 ppm immediately below the pegmatite in the footwall dolerite. In the hanging-wall dolerite, Co concentrations are between 47 and 49 ppm. Vanadium concentrations are in the range 183 to 187 ppm in the hanging wall, in contrast to a range from 196 to 206 ppm in the immediate footwall of the pegmatite, and 193 ppm in sample SB12, 14 m below the pegmatite. The gener-

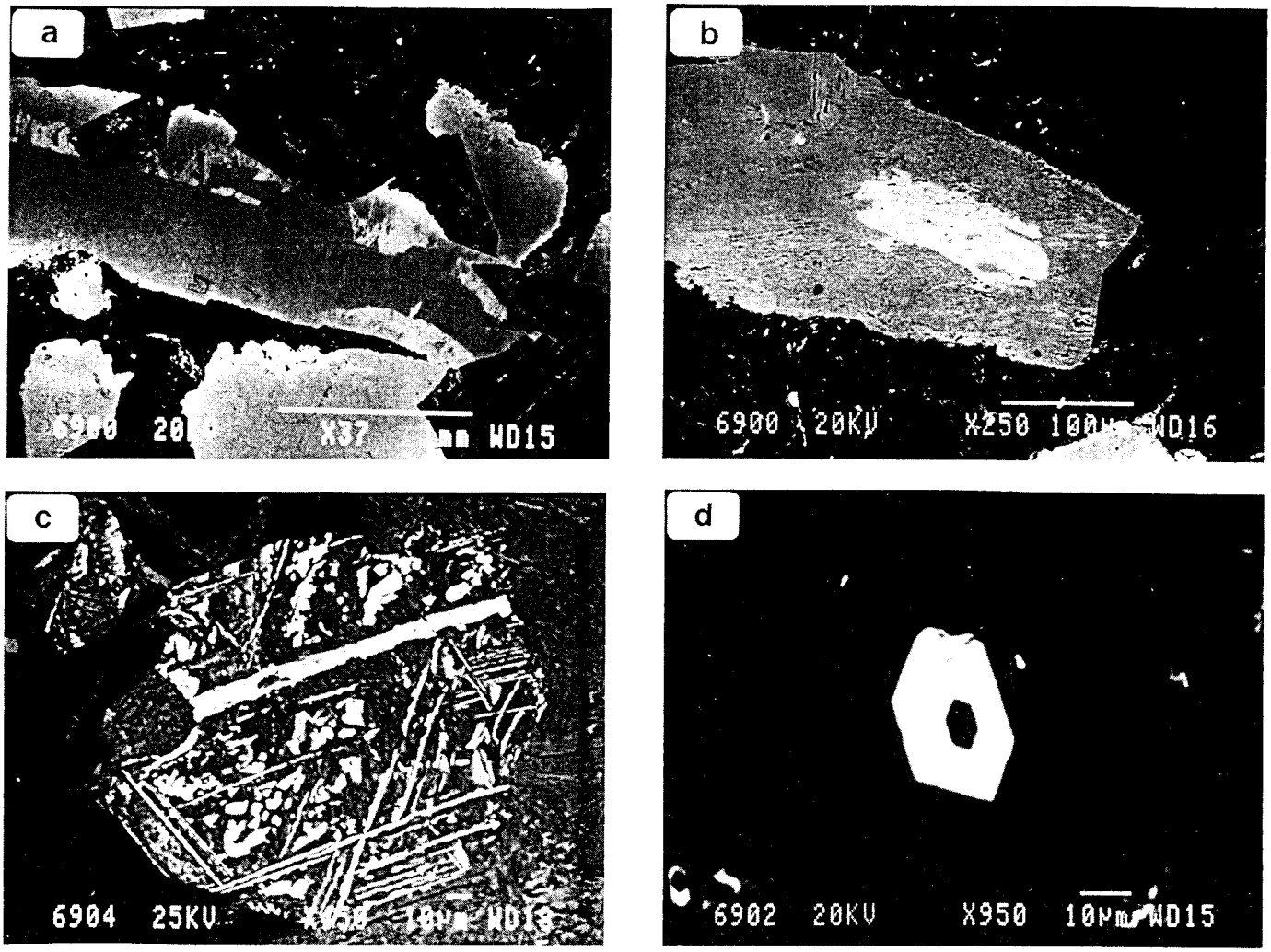

Figure 4 Backscattered electron (BSE) images of dolerite segregation pegmatite. **a)** Ferroaugite (Mg# 0.42) in the core of an augite grain (Mg# 0.69) in segregation pegmatite sample SB5. **b)** The Fe-enriched margin of a large augite grain in segregation pegmatite sample SB13. **c)** Relict skeletal ilmenite exsolution lamellae after alteration of the magnetite host, forming a geometric pattern in secondary amphibole (uralitization) on the margin of an augite grain (sample SB13). **d)** Apatite forming an overgrowth on a tiny (< 1 µm) euhedral quartz grain, in the interstitial granophyre in the segregation pegmatite (sample SB13).

Table 2 Whole-rock major- and trace-element analyses

	SB1	SB2	SB3	SB4	SB5	SB6	SB7	SB8	SB9	SB10	SB11	SB12	SB13 *
Height (m)	14.59	0.50	0.28	0.00	0.00	0.00	–0.49	–2.12	–0.62	–0.74	–0.55	–14.07	–0.15
SiO_2	53.58	53.73	53.63	54.91	55.87	54.92	54.21	53.54	54.26	54.07	54.13	54.10	55.14
TiO_2	0.74	0.74	0.76	1.35	1.35	1.12	0.81	0.79	0.80	0.78	0.76	0.72	1.03
Al_2O_3	14.68	14.73	13.86	11.90	13.47	13.87	14.25	14.41	14.03	14.20	13.70	12.55	13.63
Fe_2O_3	11.20	11.01	11.51	13.97	11.90	11.60	10.67	10.38	10.67	10.42	10.55	11.14	10.80
MnO	0.17	0.17	0.17	0.20	0.16	0.16	0.16	0.16	0.16	0.16	0.17	0.17	0.17
MgO	7.56	7.60	7.85	4.81	3.95	5.11	7.40	7.34	7.61	7.44	8.16	10.45	5.25
CaO	8.38	8.39	8.25	8.26	7.89	8.61	8.79	9.24	8.75	8.75	8.88	7.40	9.37
Na_2O	2.47	2.47	2.30	2.89	2.77	2.88	2.60	2.49	2.55	2.53	2.40	2.28	2.35
K_2O	0.76	0.73	0.65	0.95	0.96	0.82	0.81	0.72	0.76	0.77	0.68	0.58	0.60
P_2O_5	0.10	0.11	0.11	0.20	0.21	0.17	0.13	0.11	0.10	0.11	0.12	0.11	0.17
LOI	0.22	0.21	0.43	0.34	0.83	0.57	0.25	0.31	0.29	0.33	0.28	0.22	1.27
H_2O-	0.31	0.28	0.30	0.20	0.41	0.33	0.26	0.26	0.23	0.22	0.23	0.21	0.18
TOTAL	100.16	100.16	99.80	99.97	99.37	100.19	100.35	99.76	100.21	99.79	100.05	99.94	99.94
Nb	3.8	3.8	4.8	8.6	9.6	7.2	5.9	4.7	4.6	4.8	5.2	3.1	7.4
Zr	74	74	78	133	145	116	80	73	81	83	79	72	113
Y	20.7	21.2	22.3	38.0	38.0	31.3	23.7	20.6	22.8	21.5	22.3	19.8	31.0
Sr	248	247	235	205	227	228	240	239	234	240	222	207	231
Rb	24	23	20	28	29	22	24	22	23	23	20	18	18
Zn	97	97	108	125	119	113	91	97	94	93	89	97	95
Cu	95	92	93	59	48	66	70	80	76	73	74	69	54
Ni	133	132	137	57	49	73	119	120	121	125	141	177	76
Co	48	48	49	47	39	40	45	46	46	44	46	53	38
Cr	368	365	379	35	33	100	331	297	343	336	486	680	142
V	185	183	187	324	272	249	201	206	197	196	201	193	231
Sc	22.0	21.5	22.4	29.6	23.0	24.1	23.6	23.8	23.2	23.1	23.9	22.4	25.3
Ba	224	221	209	330	337	284	231	217	224	230	220	191	245

ally elevated levels of chalcophile elements in the hanging-wall dolerite suggest slightly elevated sulphide contents, possibly due to assimilation of sulphur from the Pietermaritzburg shale country rock, which contains numerous cubes of limonite after pyrite where exposed within the quarry. Low vanadium concentrations in the hanging wall relative to the footwall conflict with the relatively higher absolute normative magnetite contents and magnetite/(magnetite+ilmenite) ratios in the hanging wall, since vanadium typically partitions into magnetite rather than ilmenite. The explanation for this may be that some of the Fe assigned to normative magnetite in the hanging-wall dolerite actually resides in pyrite, thus reinforcing the possibility of sulphur assimilation.

Footwall dolerite samples more than 1 m from the pegmatite (SB8 and SB12) have Zr contents of 73 ppm and 72 ppm. Samples less than 1 m from the footwall contact, however, have Zr concentrations of 79 – 83 ppm. In the hanging wall of the pegmatite, samples S1 and S2 contain 74 ppm Zr, whereas sample S3, less than 0.5 m from the upper contact of the pegmatite, contains 78 ppm Zr. Patterns of relative enrichment in the immediate footwall of the pegmatite are also evident in the cases of Y, Nb, and Ba.

Segregation pegmatite

The evolved nature of the pegmatite is evident in substantially lower MgO contents (less than 5.3 wt.%) relative to the host dolerite (in excess of 7.3 wt.% MgO). By contrast, Na_2O, K_2O, TiO_2, and P_2O_5 are enriched in the pegmatite.

High concentrations of the incompatible trace elements (Zr, Y, Nb, and Ba) identify the pegmatite as an evolved, late-crystallizing feature. The pegmatite is also noticeably enriched in vanadium. Although depleted in the chalcophile elements Ni and Cu relative to the footwall and hanging-wall host dolerite, the main stratiform pegmatite is slightly enriched in Zn (Figure 3), which is reflected in the presence of minor sphalerite. The pegmatite pod below the main pegmatite layer is, however, not enriched in Zn.

Inter-element variations

Inter-element plots including incompatible elements (TiO_2 versus Y and Zr versus Y) and compatible elements (Ni versus MgO and Cr versus MgO), and combining data from both the segregation pegmatite and the host dolerite produce linear arrays with remarkably good correlation coefficients (Figure 6). The linear arrays in the incompatible element plots, furthermore, come close to passing through the origin. The plots

Table 3 Mineral analyses (EDS)

Pyroxene analyses

	SB1	SB1	SB1	SB8	SB8	SB8	SB8	SB6	SB6	SB5	SB5	SB5	SB5	SB13	SB13	SB13
	#1 core	#2 core	#3 core	#1marg	#1 core	#2 core	#3 core	#1 core	#2 core	#2 host	#2 core	#1 core	#3 core	#1 core	#2 core	#3 marg
SiO2	52.70	50.64	51.94	53.80	54.60	53.43	52.01	52.24	52.32	51.88	50.43	50.68	51.96	52.48	50.13	50.62
TiO2	0.15	0.20	0.45	0.34	0.14	0.35	0.36	0.54	0.33	0.68	0.24	0.61	0.61	0.55	0.26	0.35
Al2O3	0.63	1.64	1.23	0.83	1.16	1.76	1.10	1.63	1.59	1.82	1.29	1.45	1.55	1.66	3.16	1.42
FeO	24.12	18.14	12.36	15.04	13.78	9.64	11.74	11.25	11.76	12.14	19.93	13.83	12.01	9.14	10.76	16.89
MnO	0.32	0.41	0.02	0.54	0.41	0.18	0.27	0.46	0.20	0.18	0.57	0.25	0.45	0.03	0.37	0.92
MgO	16.30	11.19	15.65	25.95	27.49	18.51	15.99	15.46	15.87	14.85	8.00	14.20	14.80	16.05	14.00	9.92
CaO	5.19	17.28	18.27	2.13	1.99	15.99	17.33	18.61	17.68	18.83	18.01	17.96	18.30	18.96	19.53	20.11
Na2O	0.37	0.75	0.33	0.41	0.06	0.34	0.66	0.65	0.24	0.47	0.41	0.73	0.44	0.41	0.35	0.44
Total	99.78	100.24	100.25	99.04	99.63	100.20	99.46	100.84	99.99	100.85	98.88	99.71	100.12	99.28	98.56	100.67
Mg#	0.55	0.52	0.69	0.75	0.78	0.77	0.71	0.71	0.71	0.69	0.42	0.65	0.69	0.76	0.70	0.51

Amphibole analyses

	SB5	SB5	SB6	SB13
	#1 marg	#1 marg	#2 marg	#1 marg
SiO2	47.03	47.4	45.2	45.24
TiO2	0.81	0.05	1.61	1.61
Al2O3	3.97	3.72	5.86	6.44
FeO	24.51	32.5	24.27	23.26
MnO	0.23	0.37	0.22	0.55
MgO	7.29	2.66	7.22	8.2
CaO	12.00	10.04	10.15	10.04
Na2O	1.58	1.16	1.96	2.12
K2O	0.36	0.11	0.75	0.63
TOTAL	97.78	98.01	97.24	98.09

Plagioclase analyses

	SB5	SB5	SB5	SB6	SB6	SB13	SB13	SB8	SB8
	#1	#2	#3	#1	#2	#1	#2	#1	#2
SiO2	55.65	52.52	66.41	55.64	55.78	52.59	53.73	52.69	53.21
TiO2	0.01	0.02	0.27	0.08	0.24	0.01	0.08	0.27	0.07
Al2O3	28.51	30.17	20.27	27.30	28.04	29.87	28.81	29.94	30.00
FeO	0.93	0.48	0.46	0.59	0.69	0.51	1.07	0.88	0.60
CaO	9.95	11.87	0.53	8.98	10.09	11.94	11.26	12.08	11.80
Na2O	6.04	4.74	5.19	6.37	6.02	4.57	5	4.74	4.73
K2O	0.33	0.06	8.56	0.32	0.21	0.22	0.22	0.25	0.19
TOTAL	101.42	99.86	101.69	99.28	101.07	99.71	100.17	100.85	100.60
An/(An+Ab)	0.48	0.58	0.05	0.44	0.48	0.59	0.55	0.58	0.58

of Y versus TiO_2 and Y versus Zr are similar to one another, with pegmatite samples SB4 and SB5 the most fractionated, and SB6 and SB13 slightly less so. The host dolerite samples plot in a fairly tight cluster, with sample SB12 the least fractionated. If it is assumed that the early-crystallizing silicates excluded the elements Y, Zr, and Ti, their bulk composition would plot at the origin in each case. Simple lever rule calculations, using the end points of the cumulate data cluster to represent the possible compositional range of the parental liquid, indicate that pegmatite samples SB6 and SB13 represent between 22 and 35% crystallization of the parent liquid, and SB4 and SB5 between 39% and 48% crystallization. The values for the latter two samples are particularly high, and are probably due to modal variation within the pegmatite. They therefore do not represent the liquid that originally segregated from the underlying dolerite.

The compatible element plots (Cr versus MgO and Ni versus MgO) also suggest a fractionation origin for the pegmatite, producing linear trends with correlation coefficients > 0.98 (Figure 6). Fractionation is more difficult to model with the compatible elements than with the incompatibles, however, since some estimate of the compositions and proportions of the fractionating phases is required. Since such estimates would be equivocal, at best, and are unlikely to improve on the results obtained from the incompatible element data, no attempt has been made to model the compatible element data. The fractionation calculations are primarily of value in that they indicate the dominant influence of fractionation in the formation of the pegmatites. Similar calculations suggest segregation of the pegmatite liquid after 26 to 33% crystallization in thick basaltic lava flows (Puffer & Horter, 1993; Philpotts *et al.*, 1996).

Discussion and conclusions

The stratiform segregation pegmatite in the Natal Crushers Quarry conforms petrographically to descriptions in the existing literature from other Karoo dolerite occurrences (e.g. Mountain, 1960, p. 144), and is similar in many respects to segregation pegmatites from dolerite sheets and basalt lava flows in general (Puffer & Horter, 1993; Philpotts *et al.*, 1996). It has a sharp contact with its hanging wall, in the form of a laterally persistent sub-horizontal joint, but the footwall contact, by contrast, varies from sharp to gradational over a few millimetres. In the footwall dolerite, there are isolated small pods of pegmatite within 0.5 m of the lower contact of the main stratiform pegmatite. The small pegmatite pods, although petrographically similar to the main pegmatite body, are less fractionated.

Geochemical evidence, in the form of incompatible element ratios (Zr/Y, TiO_2/Y), is that the pegmatite and its footwall and hanging-wall host dolerite are consanguinous. There are, however, differences between the hanging-wall and foot-

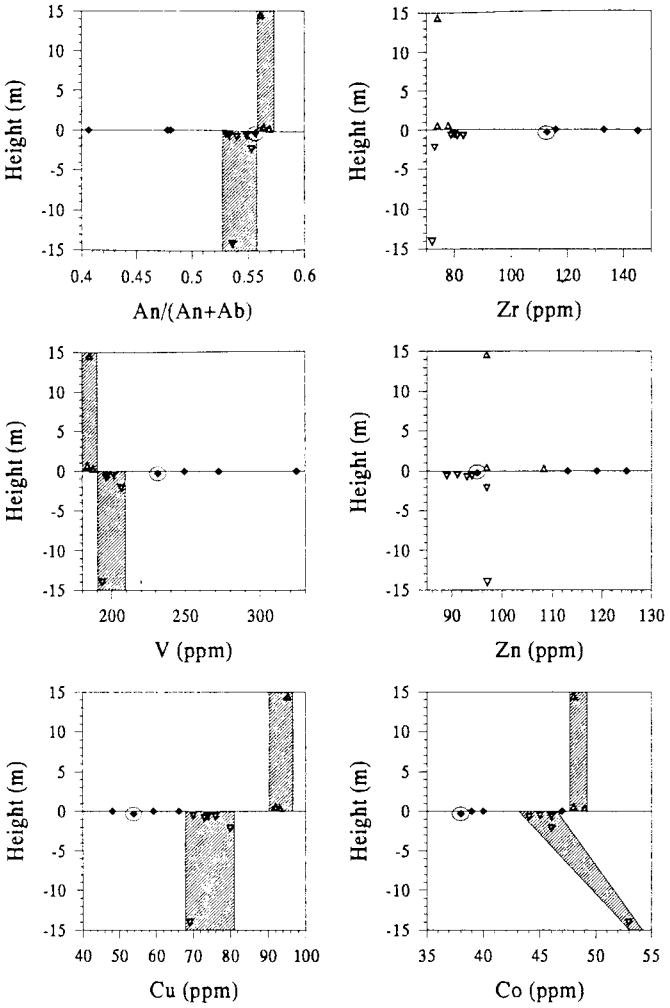

Figure 5 Plots of CIPW normative An/(An+Ab) and concentrations of Zr, V, Zn, Cu, and Co versus stratigraphic height. Filled diamonds represent the segregation pegmatite, triangles the hanging-wall dolerite, and inverted triangles the footwall dolerite.

wall dolerite. These differences are particularly evident in respect of the chalcophile elements.

The development of segregation pegmatite in the upper 50% of a mafic intrusive sheet or lava flow is usually ascribed to fractionation within a single body of magma, due to the accumulation of fractionated liquids beneath the solidification front advancing from the roof of the intrusion (Puffer & Horter, 1993; Philpotts *et al.*, 1996). This interpretation accords with the geochemical data available in this study. More calcic plagioclase and lower whole-rock V concentrations in the hanging-wall dolerite relative to the footwall (Figure 5), for example, indicate limited fractionation in the rapidly advancing solidification front in the upper part of the intrusion. Further evidence in support of this model comes from inter-element variation diagrams (Figure 6), which indicate the consanguinity of the hanging-wall and footwall dolerites and the segregation pegmatite. Even the relative sulphide depletion in the footwall dolerite (Figure 5) may be due to early segregation of sulphides at the (unexposed) base of the intrusion. Field evidence, however, presents a possible alternative to the conventional interpretation of the data.

The sharp, jointed upper contact between the pegmatite and its hanging wall suggests the possibility that the host dolerite sheet is the product of successive injections of magma which, although consanguinous, have slightly different histories. The initial injection of magma formed the hanging wall and, although chilled at its top contact with the Pietermaritzburg Formation Shales, assimilated small amounts of sulphide from its country rock. The initial intrusion needs only to have been partially solidified, and thus still hot, at the time of injection of the subsequent pulse of magma, which formed the footwall dolerite. At a crystallinity of as little as 25 – 30%, the upper magma would have had considerable yield strength (Ryerson *et al.*, 1988; Mangan & Marsh, 1992; Philpotts & Carroll, 1996), and would thus not have mixed readily with a subsequent influx of magma, but would have provided significant thermal insulation from the country rock. The footwall, insulated from the country rock by the overlying initial phase of intrusion, would have been capable of some degree of fractionation before solidification, although the presence of significant quantities of interstitial granophyre in even the most primitive samples investigated suggests that fractionation was inefficient. Late-stage rejected solute, accumulated at the interface between the two magma batches, ultimately crystallized to form the stratiform pegmatite. Small (< 0.5 m diameter) pods of pegmatite within 0.5 m of the lower contact of the main stratiform pegmatite are less evolved, geochemically and mineralogically, than the main body, and represent arrested stages of the segregation process.

The process by which rejected solute segregates and migrates to the place of formation of a pegmatite is a matter of debate. Puffer & Horter (1993) suggested, on the evidence of the vesicular nature of the Columbia River Basalt flows

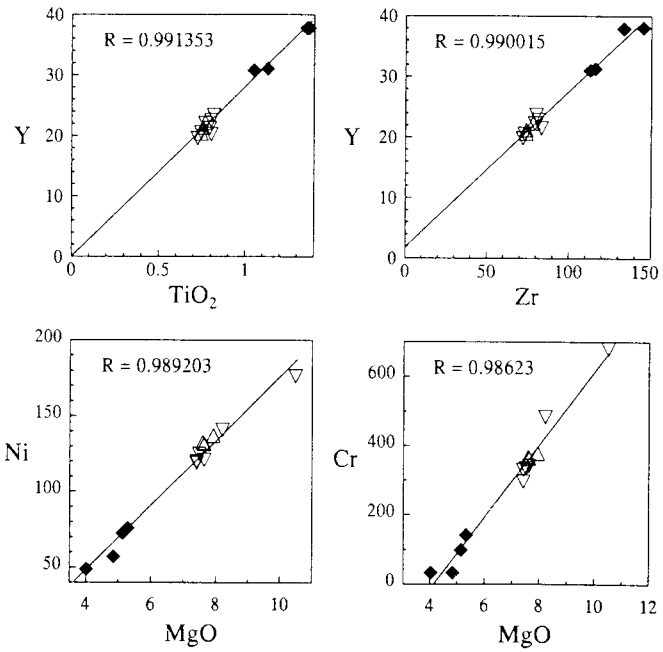

Figure 6 Inter-element plots of Y versus TiO_2, Y versus Zr, Ni versus MgO and Cr versus MgO. Major-element oxides are in weight %, trace elements in parts per million. Filled diamonds represent the segregation pegmatite, triangles the hanging-wall dolerite, and inverted triangles the footwall dolerite. The line through the data in each case is the linear regression line, the correlation coefficient (R) for which is given on the diagram.

they studied, that the upward movement of late-stage liquids was aided by rising vapour bubbles. The Natal Crushers dolerite, however, is not at all vesicular, and so it would be difficult to invoke substantial involvement of a vapour phase in this case. Philpotts *et al.* (1996) ascribed segregation pegmatites in basalt flows to filter pressing as a result of crystal-mush compaction. Evidence against filter pressing in the Natal Crushers dolerite is the consistently high proportion of interstitial granophyre throughout the sequence studied. Larsen & Brooks (1994) followed McBirney (1987; 1989) in suggesting that the gabbroic pegmatites in the Skaergaard Intrusion crystallized from light rejected solute produced by pyroxene-dominated fractionation (e.g. Sparks & Huppert, 1984; Morse, 1986). With their buoyancy enhanced by dissolved H_2O (McBirney & Sonnenthal, 1990), the late-stage liquids were postulated by Larsen & Brooks (1994) to have migrated upward through the crystallizing dolerite by a process of compositional convection (Sparks *et al.*, 1985). The authors believe the pegmatite in the Natal Crushers dolerite crystallized from liquids segregated by processes similar to those outlined by Larsen & Brooks (1994).

Segregation pegmatites in relatively small dolerite intrusive sheets and basalt lava flows do not display the degree of evolution displayed by those in large layered mafic complexes, and can perhaps legitimately be regarded as incipient forms of pegmatite phenomena seen in the larger intrusions. Where pegmatites occur within bodies that are demonstrably single intrusions or lava flows, it is common for the rejected solute from which the pegmatites crystallized to have migrated to the base of the solidification front advancing from the top contact of the body (Puffer & Horter, 1993; Philpotts *et al.*, 1996). The case illustrated here perhaps takes the process a step further, in that there is evidence of upward migration of fractionated liquids to the interface between two successive magma intrusions, albeit of similar and relatively unfractionated compositions. There is thus an approach to the situation pertaining in large layered complexes, where late-stage liquids migrate (upwards or downwards) until they are trapped by impenetrable cumulate boundaries, or reach levels of neutral buoyancy, before crystallizing as pegmatites (Larsen & Brooks, 1994; Scoon & Mitchell, 1994).

The pegmatites of the Skaergaard intrusion (Larsen & Brooks, 1994) display a pronounced and progressive internal zonation within individual pegmatite bodies, ultimately providing evidence of possible silicate liquid immiscibility between a granophyric liquid and a mafic liquid. The Skaergaard pegmatites change geometry from discordant podiform bodies in the Lower Zone and lower part of the Middle Zone to semi-conformable sheets in the upper part of the Middle Zone and in the Upper Zone. They are believed to have crystallized from upward-migrating, relatively buoyant liquids, their geometry being controlled in places by impenetrable cumulate layers which prevented further upward migration of the liquid. In this latter respect, the Natal Crushers pegmatite has something in common with the pegmatites in the Middle and Upper Zones of the Skaergaard intrusion, but it is a smaller-scale, less evolved feature, commensurate with the relative sizes of the intrusions.

Acknowledgements

The management of Anglo Alpha Ltd, and in particular Mr W. Arnold and Mr H. Rozenkrantz, are thanked for their assistance in the completion of this project and for permission to publish the results. Photographic material was processed at the University of Durban-Westville by Mr A. Rajh. This work was supported by research funding from the University of Durban-Westville and from the Foundation for Research Development. Stephen Johnston is thanked for an informal review of the draft manuscript, and A.R. Philpotts and F.J. Kruger are thanked for constructive reviews that improved the final product.

References

Eales, H.V. (1959). The Khale dolerite sheet. *Trans. geol. Soc. S. Afr.*, **62**, 81–109.

---- & Booth, P.W.K. (1974). The Birds River Gabbro Complex, Dordrecht district. *Trans. geol. Soc. S. Afr.*, **77**, 1–15.

Encarnación, J., Fleming, T.H., Elliot, D.H. & Eales, H.V. (1996). Synchronous emplacement of Ferrar and Karoo dolerites and the early breakup of Gondwanaland. *Geology*, **24**, 535–538.

Jahns, R.H. & Burnham, C.W. (1969). Experimental studies of pegmatite genesis: I. A model for the derivation and crystallization of granitic pegmatites. *Econ. Geol.*, **64**, 843–864.

Larsen, R.B. & Brooks, C.K. (1994). Origin and evolution of gabbroic pegmatites in the Skaergaard intrusion, east Greenland. *J. Petrol.*, **35**, 1651–1679.

Linström, W. (1987). Die geologie van die gebied Durban. *Expl. Sheet 2930 (Durban), Geol. Surv. S. Afr.*, 33 pp.

Mangan, M.T. & Marsh, B.D. (1992). Solidification front fractionation in phenocryst-free sheet-like magma bodies. *J. Geol.*, **100**, 605–620.

McBirney, A.R. (1987). Constitutional zone refining. *In*: Parsons, I (Ed.), *Origins of Igneous Layering*. Reidel, London, 437–452.

---- (1989). The Skaergaard Layered Series: 1. Structure and average compositions. *J. Petrol.*, **30**, 363–399.

---- & Sonnenthal, E.L. (1990). Metasomatic replacement in the Skaergaard Intrusion, East Greenland: preliminary observations. *Chem. Geol.*, **88**, 245–260.

Morse, S.A. (1986). Convection in aid of adcumulus growth. *J. Petrol.*, **27**, 1183–1214.

Mountain, E.D. (1960). Felsic material in Karroo dolerite. *Trans. geol. Soc. S. Afr.*, **63**, 137–151.

Naicker, S.B. (1996). *The petrology and geochemistry of dolerite pegmatite at Natal Crushers quarry*. B.Sc. (Hons.) dissertation (unpubl.), Univ. Durban-Westville, 21 pp.

Norrish, K. & Hutton, J.T. (1969). An accurate X-ray spectrographic method for the analysis of a wide range of geological samples. *Geochim. Cosmochim. Acta*, **33**, 431–453.

Philpotts, A.R. & Carroll, M. (1996). Physical properties of partly melted tholeiitic basalt. *Geology*, **24**, 1029–1032.

----, ---- & Hill, J.M. (1996). Crystal-mush compaction and the origin of pegmatitic segregation sheets in a thick flood-basalt flow in the Mesozoic Hartford basin, Connecticut. *J. Petrol.*, **37**, 811–836.

Puffer, J.H. & Horter, D.L. (1993). Origin of pegmatitic segregation veins within flood basalts. *Bull. Geol. Soc. Am.*, **105**, 738–748.

Randall, B.A.O. (1989). Dolerite-pegmatites from the Whin Sill near Barrasford, Northumberland. *Proc. Yorkshire Geol. Soc.*, **47**, 249–265.

Ryerson, F.J., Weed, H.C. & Piwinskii, A.J. (1988). Rheology of subliquidus magmas 1. Picritic compositions. *J. Geophys. Res.*, **93**, 3421–3436

Scoon, R.N. & Mitchell, A.A. (1994). Discordant iron-rich ultramafic pegmatites in the Bushveld Complex and their relationship to iron-rich intercumulus and residual liquids. *J. Petrol.*, **35**, 881–917.

Shirley, D.N. (1987). Differentiation and compaction in the Palisades Sill, New Jersey. *J. Petrol.*, **28**, 835–865.

Sparks, R.S.J. & Huppert, H.E. (1984). Density changes during fractional crystallization of basaltic magmas: fluid dynamic implications. *Contrib. Mineral. Petrol.*, **85**, 300–309.

----, ----, Kerr, R.C., McKenzie, D.P. & Tait, S.R. (1985). Postcumulus

processes in layered intrusions. *Geol. Mag.*, **122**, 555–568.

Tomkeieff, S.I. (1929). A contribution to the petrology of the Whin Sill. *Mineral. Mag.*, **22**, 100–120.

Walker, F. & Poldervaart, A. (1949). Karoo dolerites of the Union of South Africa. *Bull. Geol. Soc. Am.*, **60**, 591–706.

Wilhelm, S. & Wörner, G. (1996). Crystal size distribution in Jurassic Ferrar flows and sills (Victoria Land, Antarctica): Evidence for processes of cooling, nucleation, and crystallization. *Contrib. Mineral. Petrol.*, **125**, 1–15.

Williams, C.M. (1995). *Petrogenesis of the New Amalfi sheet: a highly differentiated Karoo intrusion*. M.Sc. thesis (unpubl.), Rhodes Univ., Grahamstown, 192 pp.

Editorial control: R.G. Cawthorn.